Atmos. Chem. Phys., 17, 7127–7142, 2017
https://doi.org/10.5194/acp-17-7127-2017

Atmospheric Chemistry and Physics
Open Access
EGU

How the OH reactivity affects the ozone production efficiency: case studies in Beijing and Heshan, China

Yudong Yang[1], Min Shao[1], Stephan Keßel[2], Yue Li[1], Keding Lu[1], Sihua Lu[1], Jonathan Williams[2], Yuanhang Zhang[1], Liming Zeng[1], Anke C. Nölscher[2,a], Yusheng Wu[1,b], Xuemei Wang[3], and Junyu Zheng[4]

[1]State Joint Key Laboratory of Environmental Simulation and Pollution Control, College of Environmental Science and Engineering, Peking University, Beijing, China
[2]Department of Atmospheric Chemistry, Max Plank-Institute for Chemistry, Mainz, Germany
[3]School of Atmospheric Science, Sun Yat-Sen University, Guangzhou, China
[4]School of Environmental Science and Engineering, South China University of Technology, Guangzhou, China
[a]now at: Division of Geological and Planetary Sciences, California Institute of Technology, Pasadena, CA, USA
[b]now at: Department of Physics, University of Helsinki, Helsinki, Finland

Correspondence to: Min Shao (mshao@pku.edu.cn)

Received: 23 June 2016 – Discussion started: 15 July 2016
Revised: 14 April 2017 – Accepted: 19 April 2017 – Published: 15 June 2017

Abstract. Total OH reactivity measurements were conducted on the Peking University campus (Beijing) in August 2013 and in Heshan (Guangdong province) from October to November 2014. The daily median OH reactivity was $20 \pm 11\,s^{-1}$ in Beijing and $31 \pm 20\,s^{-1}$ in Heshan, respectively. The data in Beijing showed a distinct diurnal pattern with the maxima over $27\,s^{-1}$ in the early morning and minima below $16\,s^{-1}$ in the afternoon. The diurnal pattern in Heshan was not as evident as in Beijing. Missing reactivity, defined as the difference between measured and calculated OH reactivity, was observed at both sites, with 21 % missing reactivity in Beijing and 32 % missing reactivity in Heshan. Unmeasured primary species, such as branched alkenes, could contribute to missing reactivity in Beijing, especially during morning rush hours. An observation-based model with the RACM2 (Regional Atmospheric Chemical Mechanism version 2) was used to understand the daytime missing reactivity in Beijing by adding unmeasured oxygenated volatile organic compounds and simulated intermediates of the degradation from primary volatile organic compounds (VOCs). However, the model could not find a convincing explanation for the missing reactivity in Heshan, where the ambient air was found to be more aged, and the missing reactivity was presumably attributed to oxidized species, such as unmeasured aldehydes, acids and dicarbonyls. The ozone production efficiency was 21 % higher in Beijing and 30 % higher in Heshan when the model was constrained by the measured reactivity, compared to the calculations with measured and modeled species included, indicating the importance of quantifying the OH reactivity for better understanding ozone chemistry.

1 Introduction

Studies on total OH reactivity in the atmosphere have been of increasing interest over the last two decades. The instantaneous total OH reactivity is defined as

$$k_{OH} = \sum_i k_{OH+X_i}[X_i], \quad (1)$$

where X represents a reactive species (CO, NO_2, etc.) and k_{OH+X_i} is the rate coefficient for the reaction between X and OH radicals. Total OH reactivity is an index for evaluating the amounts of reductive pollutants in terms of ambient OH loss and hence their roles in atmospheric oxidation (Williams, 2008; Williams and Brune, 2015; Yang et al., 2016). It also provides a constraint for OH budget calculation in both field campaigns and laboratory studies (Stone et al., 2012; Fuchs et al., 2013).

Total OH reactivity measuring techniques, e.g., two laser-induced fluorescence (LIF)-based techniques (Calpini et al.,

Table 1. Total OH reactivity measurements in urban areas.

Campaign	Site	Year	Method	$k_{OH(measured)}$ (s^{-1})[a]	$k_{OH(calculated)}$ (s^{-1} if it is a value)[b]	Measured species[c]	Reference
SOS	Nashville, TN, USA	summer 1999	LIF flow tube	11.3	7.2	SFO	Kovacs et al. (2003); Kovacs and Brune (2001)
PMTACS-NY 2001	New York, NY, USA	summer 2001	LIF flow tube	15–25	within 10 %	SFO	Ren et al. (2003)
PMTACS-NY 2004	New York, NY, USA	winter 2004	LIF flow tube	18–35	statistically lower	SF	Ren et al. (2006a)
MCMA-2003	Mexico City, Mexico	spring 2003	LIF flow tube	10–120	30 % less than	–	Shirley et al. (2006)
TexAQS	Houston, TX, USA	summer 2000	LIF flow tube	7–12	agree well	SFO	Mao et al. (2010)
TRAMP2006	Houston, TX, USA	summer 2006	LIF flow tube	9–22	agree well	SFOB	Mao et al. (2010)
	Tokyo, Japan	2003–2004	LP-LIF	10–100	30 % less than	SFOB	Sadanaga et al. (2004); Yoshino et al. (2006)
	Tokyo, Japan	summer 2006	LP-LIF	10–55	30 % less than	SFOB	Chatani et al. (2009)
	Tokyo, Japan	spring 2009	LP-LIF	10–35	22 % less than	SFOB	Kato et al. (2011)
	Tokyo, Japan	winter 2007, autumn 2009	LP-LIF	10–80	10–15 less than	SFOB	Yoshino et al. (2012)
	Mainz, German	summer 2005	CRM	10.4		–	Sinha et al. (2008)
MEGAPOLI	Paris, France	winter 2010	CRM	10–130	10–54 % less than	SO	Dolgorouky et al. (2012)
ClearfLo	London, England	summer 2012	LP-LIF	10–116	20–40 %	SFOB	Whalley et al. (2016)
	Lille, France	autumn 2012	CRM, LP-LIF	∼ 70	reasonable agreement	SFO	Hansen et al. (2015)
	Dunkirk, France	summer 2014	CRM	10–130		–	Michoud et al. (2015)

[a] For sources from different studies, the measured reactivity was presented as the averaged results, ranges of diurnal variations or the ranges of the whole campaign. [b] For sources from different studies, the calculated reactivity was presented within an uncertainty range as a percentage reduction or s^{-1} reduction. [c] Measured species have been used for the calculated reactivity (following Lou et al., 2010): S indicates inorganic compounds (CO, NO_x, SO_2, etc.) plus hydrocarbons (including isoprene); F indicates formaldehyde; O indicates OVOCs other than formaldehyde; B indicates BVOCs other than isoprene. "–" indicates a lack of information regarding what has been measured or how long it has been measured.

1999; Kovacs and Brune, 2001) and one proton transfer reaction mass spectrometry (PTR-MS)-based technique, the comparative reactivity method (CRM; Sinha et al., 2008), were developed in recent years. A brief comparison of these techniques and their interferences were summarized (Yang et al., 2016). By deploying these measuring techniques, total OH reactivity measurements have been intensively conducted in urban and suburban areas. Details of these campaigns were listed in Tables 1 and 2. Most of the campaigns exhibited similar diel features with higher reactivity during dawn and rush hours of the early morning, and lower levels in the afternoon, which could be explained by the change in boundary layer height, emissions and oxidation processes. Anthropogenic volatile organic compounds (VOCs) and inorganics, such as CO and NO_x ($NO + NO_2$), are major known OH sinks in urban areas.

However, a substantial difference between measured and calculated or modeled OH reactivity, termed the missing reactivity, was revealed in most field campaigns. Compared to the high percentages of missing reactivity in forested areas (Sinha et al., 2010; Nölscher et al., 2012, 2016; Edwards et al., 2013; Williams et al., 2016), most campaigns in urban and suburban areas gave relatively lower percentages of missing reactivity, except for the 75 % missing reactivity in Paris in MEGAPOLI under the influence of continental air masses (Dolgorouky et al., 2012).

Various methods were used in exploring the origins of missing reactivity. Unmeasured primary species are important candidates. Sheehy et al. (2010) discovered a higher percentage of missing reactivity during morning rush hours and found that the unmeasured primary species, including organics with semi-volatility and low volatility, could contribute up to 10 % of total reactivity. Direct measurements of reactivity of anthropogenic emission sources, such as vehicle exhaust and gasoline evaporation, were conducted. An average of 17.5 % missing reactivity was found in vehicle exhaust measurements (Nakashima et al., 2010). For gasoline evaporation, a study showed that if primary emitted branched–chained alkenes were considered, the measured and calculated reactivity agreed (Wu et al., 2015). Besides primary emitted species, unknown secondary species were not negligible. Yoshino et al. (2006) found a good correlation between missing reactivity and measured oxygenated VOCs (OVOCs) in three seasons, except for winter, assuming that the unmeasured OVOCs could be major contributors of missing reactivity; in one case, the OVOCs could increase reactivity by over 50 % (Lou et al., 2010). The observation-based model (OBM) was widely used to evaluate the measured reactivity (Lee et al., 2010; Lou et al., 2010; Whalley et al., 2016), confirming the important contribution from OVOCs and undetected intermediate compounds.

Ground-level ozone pollution has been of increasing concern in China. While the ozone concentration exceeds Grade II of China's National Ambient Air Quality Standard (2012; 93 ppbV) frequently in summer in the Beijing–Tianjin–Hebei area and the Pearl River Delta (PRD) region (Wang et al., 2006; Zhang et al., 2008), it appears there is an increasing trend for ozone in Beijing and other areas in recent years (Zhao et al., 2009; Zhang et al., 2014). Compared to traditional empirical kinetic model approach (EKMA; Dodge et al., 1977), the OH reactivity due to VOCs (termed VOC reactivity) rather than VOC mixing ratio was used in the calculation of ozone production rate (Geddes et al., 2009; LaFranchi et al., 2011; Sinha et al., 2012; Zhang et al., 2014). Due to the limitation of current measurement techniques, some VOC species which could not be quantified so far and there-

Table 2. Total OH reactivity measurements in suburban and surrounding areas.

Campaign	Site	Year	Method	$k_{OH(measured)}$ (s^{-1})	$k_{OH(calculated)}$ (s^{-1} if it is a value)	Measured species	Reference
	Central Pennsylvania, PA, USA	spring 2002	LIF flow tube	6.1		–	Ren et al. (2005)
PMTACS-NY2002	Whiteface Mountain, NY, USA	summer 2002	LIF flow tube	5.6	within 10 %	–	Ren et al. (2006b)
TORCH-2	Weybourne, England	spring 2004	LIF flow tube	4.85	2.95	SFO	Ingham et al. (2009); Lee et al. (2010)
CAREBeijing-2006	Yufa, China	summer 2006	LP-LIF	10–30	agree well	S	Lu et al. (2010, 2013)
PRIDE-PRD	Backgarden, China	summer 2006	LP-LIF	10–120	50 % less than	S	Lou et al. (2010)
DOMINO	El Arenosillo, Spain	winter 2008	CRM	6.3–85		SF	Sinha et al. (2012)
		spring 2013	CRM	53	23	SFOB	Kumar and Sinha (2014)

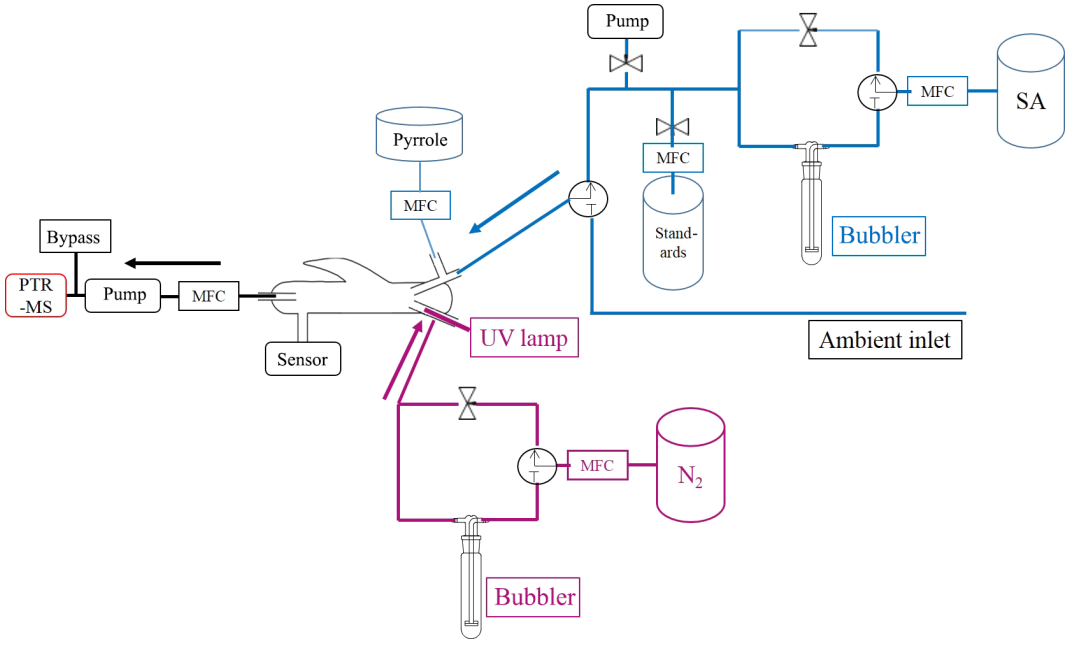

Figure 1. Schematic figures of the CRM system in Beijing and Heshan observations. The blue color represents the ambient air or synthetic air injection system; purple represents OH generating system; black represents the detection system. Pressure is measured by the sensor connected to the glass reaction.

fore cannot be integrated into current chemical mechanisms of model run, could create great uncertainty in ozone production prediction. By directly measuring the total OH reactivity, VOC reactivity can be obtained by deducting the inorganic reactivity from the total OH reactivity, which provides a constraint for evaluating the roles of reactive VOCs in air chemistry (Sadanaga et al., 2005; Sinha et al., 2012; Yang et al., 2016).

This paper presents field data in China from two intensive observations conducted in August 2013 in Beijing and October to November 2014 in Heshan, Guangdong, focusing on OH reactivity and related species. The variations of total OH reactivity at both sites were compared with similar observations in urban and suburban areas worldwide. Thereafter, a zero-dimensional box model based on the Regional Atmospheric Chemical Mechanism 2 (RACM2) was employed for OH reactivity simulations. The possible missing reactivity and its importance for the ozone production calculation are discussed.

2 Methods

2.1 Total OH reactivity measurements

2.1.1 Measurement principles

Total OH reactivity was measured by the CRM first developed at the Max Planck Institute for Chemistry (Sinha et al., 2008). The CRM system, built accordingly at Peking University, consisted of three major components: an inlet and calibration system, a reactor and a measuring system, as shown in Fig. 1. Ambient air was sampled after a Teflon filter and then pumped through a 14.9 m Teflon 3/8 in (outer diameter) inlet at a rate of about 7 L min^{-1}, with a 5–6 s residence time.

In this method, pyrrole (C_4H_5N) was used as the reference substance and was quantified by a quadrupole PTR-MS (Ionicon Analytic, Austria). There are four working modes for the measuring procedure: in the C0 mode, pyrrole (Air Liquid Ltd, USA) is introduced into the reactor with dry synthetic air (99.99 %; Chengweixin Gas Ltd, China). A mercury lamp (185nm, used for OH radicals generation) is turned off and high-purity dry nitrogen (99.99 %; Chengweixin Gas Ltd, China) is mixed into the reactor through a second arm. In this mode, the highest signals of m/z 68 (protonated mass of pyrrole) C0 are obtained. Then, in the C1 mode, the nitrogen and synthetic air are still dry but the mercury lamp is turned on. The mixing ratio of pyrrole decreases to C1. The difference between C0 and C1 is mainly due to the photolysis of pyrrole (Sinha et al., 2008). C2 mode is the "zero air" mode in which synthetic air and nitrogen are humidified before being introduced into the reactor. The photolysis of water vapor generates OH radicals which react with pyrrole in the reactor to C2 level. Then, C3 mode is the measuring mode in which the automatic valve switches from synthetic air to ambient air. The ambient air is pumped into the reactor to react with OH radicals, competing with pyrrole molecules. The mixing ratio of pyrrole is detected as C3. Total OH reactivity is calculated as below, based on equations from Sinha et al. (2008):

$$k_{OH} = c1 \times k_{Pyr+OH} \times \frac{c3 - c2}{c1 - c3}. \quad (2)$$

Ambient air or synthetic air was introduced at 160–170 mL min^{-1} with the total flow 320–350 mL min^{-1} (the typical dilution factor was about 2–2.15 depending on the situation). The residence time of air inside the reactor was less than 30 s before it was pumped by the Teflon pump. The typical C1 mixing ratios for pyrrole in Beijing and Heshan measurements were about 60 and 55 ppbV, respectively, while the mixing ratios of OH radicals generated by the mercury lamp were about 35 and 28 ppbV. The mixing ratios were quite consistent for both of the campaigns. Corrections about pseudo-first-order kinetics were conducted for both measurements, based on the methods in Sinha et al. (2008). The typical correction factors could be presented as

$$R_{true} = 0.0008 \times (R_{mea})^2 + 0.78 \times R_{mea} - 0.042 \quad (3)$$

$$R_{true} = -0.0004 \times (R_{mea})^2 + 0.81 \times R_{mea} - 0.017. \quad (4)$$

2.1.2 Calibrations and tests

We performed two calibrations for the measurements. First, PTR-MS was calibrated by diluted dry pyrrole standard gas ranging from less than 10 to over 160 ppbV (presented in Fig. S1 in the Supplement). Additionally, we conducted an intercomparison with humidified pyrrole dilution gas. The sensitivity was about 3 to 5 % higher than dry calibration, which was considered for later calculation (Sinha et al., 2009). The tests of the CRM system were done by using both the single-standard gas, such as CO, propane and propene (Huayuan Gas Ltd, China), and a standard of the mixture PAMS (photochemical assessment monitoring stations) of 56 non-methane hydrocarbons (NMHCs; SpecialGas Ltd, USA). The results of the calibrations and tests are presented in Fig. 2. Measured and calculated OH reactivity agreed well within the uncertainty for all calibrations.

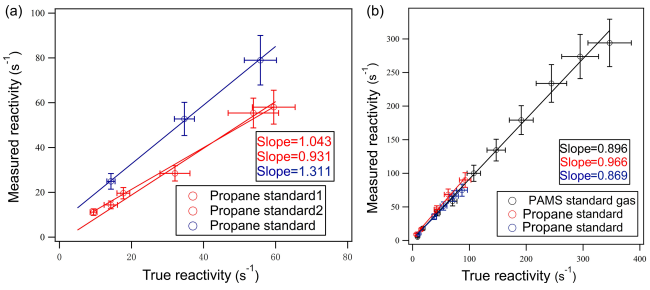

Figure 2. OH reactivity calibration in Beijing **(a)** and Heshan **(b)**. Left: calibration in Beijing using two single standards: propane and propene. Right: calibration in Heshan using three standards: propane, propene and mixed PAMS 56 non-methane hydrocarbons (NMHCs). Error bars stand for estimated uncertainty of the measured and true reactivity.

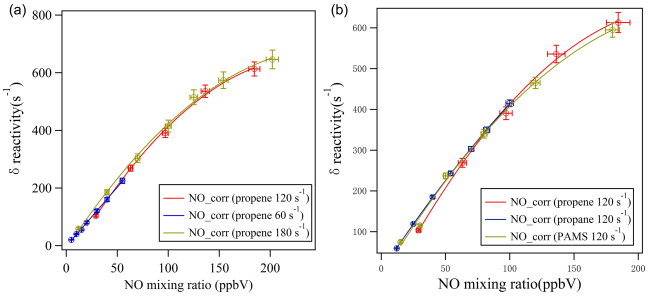

Figure 3. NO-correction experiments and fitting curves in Heshan in 2014. **(a)** NO-correction experiments with different mixing ratios of propene standard gas; **(b)** NO-correction experiments with different standard gases at the same reactivity level: 120 s^{-1}. Error bars stand for estimated uncertainty of the NO mixing ratios and difference in reactivity.

A key factor influencing the measurement results is the stability of the OH radical generator. One major interference could be the difference in relative humidity between C2 mode and C3 mode. During the experiment, we used one single-needle valve to control the flow rate of synthetic air going through the bubbler, so that the relative humidity during C2 mode could be adjusted to match humidity during ambient sampling (C3 mode). Meanwhile, the remaining minor difference could be corrected by factors derived from the OH reactivity–humidity correction experiment. The details of the OH-correction experiment and the data were presented in the supporting information (Figs. S1 and S2).

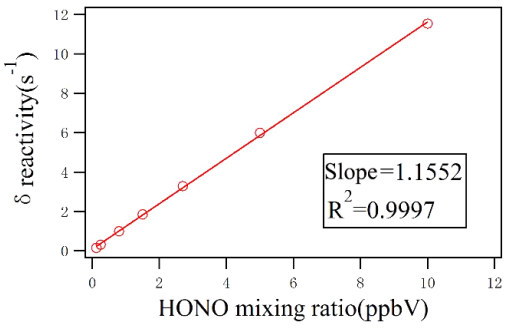

Figure 4. Nitrous acid (HONO)-correction experiments and the fitting curve in Heshan in 2014.

The other interference might be caused by ambient NO, which produces additional OH radicals via recycling of HO_2 radicals (Sinha et al., 2008; Dolgorouky et al., 2012; Michoud et al., 2015). The amount of OH radicals through this pathway is hard to quantify. During the morning rush hours or on polluted cloudy days, NO levels could rise to over 30 ppbV in both Beijing and Heshan, which could then potentially introduce high uncertainties for measurements. The NO-correction experiments were conducted by introducing given amounts of VOC standard gases into the reactor. When the stable concentrations for C2 were reached, different levels of NO were injected into the reactor and the "measured" reactivity decreased as the NO mixing ratio increased. Then, a correction curve was fitted between the differences in reactivity and NO mixing ratios. Several standard gases and different levels of base reactivity (from less than 30 to over 180 s^{-1}) have been tried and the curve was quite consistent for all tested gases, as shown in Fig. 3. The correction derived from the curve was used later to correct ambient measurements according to simultaneous detected NO levels. The correction was necessary when NO mixing ratio was larger than 5 ppbV, which was quite often observed in the morning as well as on cloudy days in Beijing and Heshan. The relative change for reactivity results could be over 100 s^{-1} when NO mixing ratio was about 30 ppbV.

A further potential interference comes from nitrous acid (HONO). The photolysis of HONO in the reactor could generate the same amount of OH radicals and NO molecules, as shown in R1. The additional OH radicals and NO molecules can be both interferences with the reactivity measurements. Similar correction experiments were conducted as the NO-correction experiment. HONO values were added stepwise in several mixing ratios (1–10 ppbV), generated by a HONO generator (Liu et al., 2016) and thus introduced into the reactor. A curve was fitted between the differences in reactivity and HONO mixing ratios, as presented in Fig. 4. The correction associated with this curve was also applied later in the ambient measurements.

$$\mathrm{HONO} \xrightarrow{h\gamma} \mathrm{OH} + \mathrm{NO} \qquad \text{(R1)}$$

To make sure the production of OH radicals was stable during the experiments, C1 mode was measured for 1–2 h every other day and C2 mode was measured for 20–30 min every 2 h. With the above calibrations and tests in consideration, the detection limits of CRM methods in two campaigns were around 5 s^{-1} (2σ). The total uncertainty of the method was about 20 % (1σ) due to the rate coefficient of pyrrole reactions (15 %), flow fluctuation (3 %), instrument precision (6 % when measured reactivity was greater than 15 s^{-1}), standard gases (5 %) and corrections for relative humidity (5 %).

2.2 Field measurements

2.2.1 Measuring sites and periods

The urban measurements started from 10 to 27 August 2013 at the Peking University (PKU) site (116.18° E, 39.99° N), which was set on the roof of a six-story building. The site is about 300 m from the six-lane road to the east and 500 m from the eight-lane road to the south. This site is an urban site used for intensive field measurements of air quality in Beijing for long periods. Detailed information about this site can be found elsewhere (Yuan et al., 2012).

Suburban measurements were conducted from 20 October to 22 November 2014 at the Heshan (HS) site, Guangdong (112.93° E, 22.73° N). The site is located on top of a small hill (60 m above ground) in Jiangmen, which is 50 km from the medium-sized city of Foshan (with a population of about 7 million) and 80 km from the megacity of Guangzhou. This is the supersite for measurements of air quality trends by the Guangdong provincial government, detailed information about which can also be found in Fang et al. (2016).

2.2.2 Simultaneous measurements

During both intensive campaigns, fundamental meteorological parameters and trace gases were measured simultaneously. Meteorological parameters such as temperature, relative humidity, pressure, wind speed and wind direction were measured. NO and NO_x mixing ratios were measured by chemiluminescence (model 42i, Thermo Fisher Inc, USA), and O_3 was measured by UV absorption (model 49i, Thermo Fisher Inc, USA). CO was measured by gas filter correlation (model 48i, Thermo Fisher Inc, USA) and SO_2 was measured by pulsed fluorescence (model 43C, Thermo Fisher Inc, USA). The photolysis frequencies were measured by a spectral radiometer (SR) including eight photolysis parameters. These parameters were all averaged into 1 min resolution. The performances of these instruments were presented in Tables S1 and S2 in the Supplement.

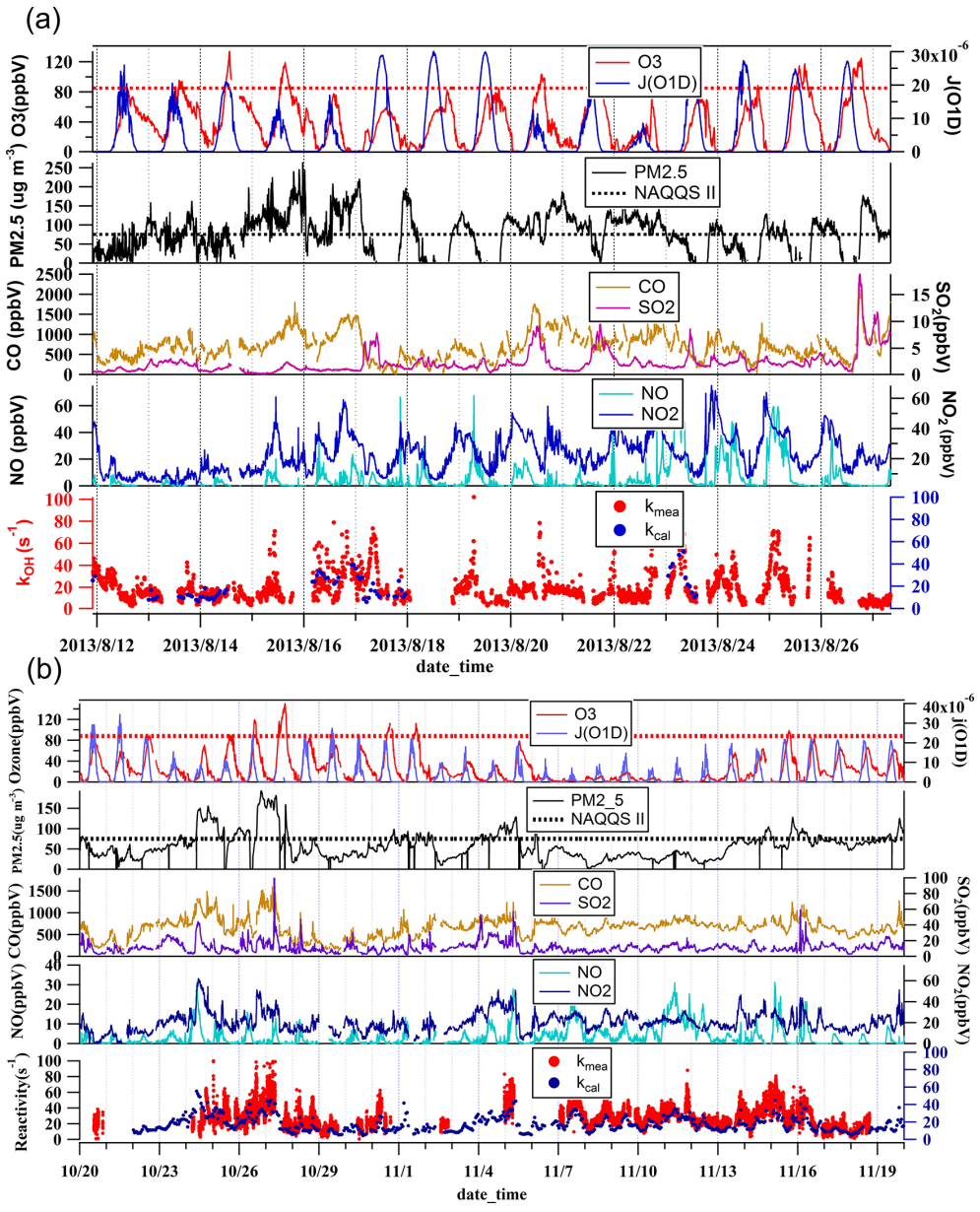

Figure 5. **(a)** Time series of meteorological parameters and inorganic trace gases during August 2013 in Beijing. Red and black dashed lines are Grade II of the National Ambient Air Quality Standard. **(b)** Time series of meteorological parameters and inorganic trace gases during October–November 2014 in Heshan. Red and black dashed lines are Grade II of the National Ambient Air Quality Standard.

VOCs were measured by a cryogen-free online GC-MSD/FID system, developed at Peking University (Yuan et al., 2012; Wang et al., 2014a). The time resolution is 1 h but the sampling time starts from the 5th to 10th minute every hour. The system was calibrated by two sets of standard gases: 56 NMHCs, including 28 alkanes, 13 alkenes and alkynes, and 15 aromatics; and EPA TO-15 standards (https://www3.epa.gov/ttnamti1/files/ambient/airtox/to-15r.pdf), including additional OVOCs and halocarbons. The detection limits ranged from 10 to 50 ppt, depending on the species. Formaldehyde was measured by the Hantzsch method with a time resolution of 1 min. Detailed information about this instrument is described in a previous paper (Li et al., 2014).

2.3 Model description

2.3.1 Box model

A zero-dimensional box model was applied to produce the unmeasured secondary products and OH reactivity for both field observations. The chemical mechanism employed in the

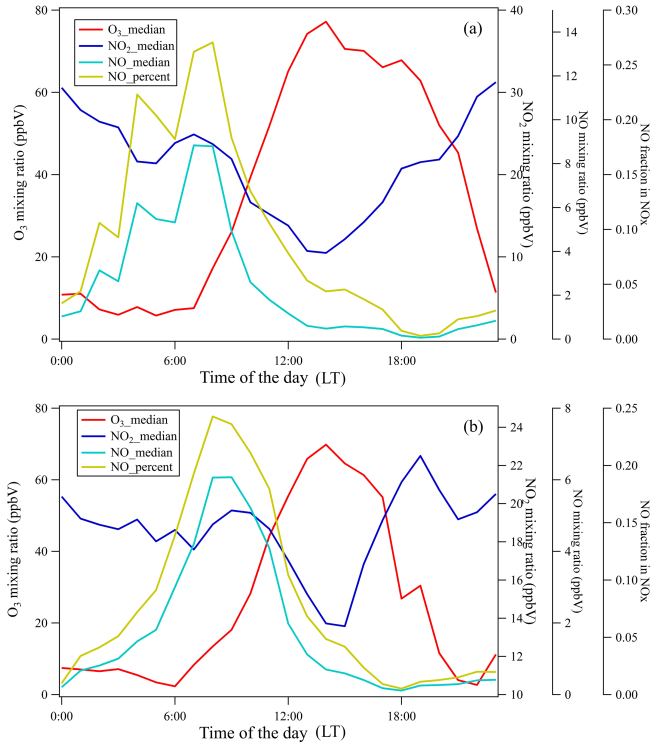

Figure 6. Diurnal variations of O_3, NO, NO_2 and relative contribution of NO to NO_x in Beijing in 2013 **(a)** and Heshan in 2014 **(b)**.

model was RACM2 (Stockwell et al., 1997; Goliff et al., 2013), with implementation of the Mainz Isoprene Mechanism (MIM; Pöschl et al., 2000) and update versions by Geiger et al. (2003) and Karl et al. (2006) for isoprene reactions. The model was constrained by measured photolysis frequencies, ancillary meteorology and inorganic gas measurements, as well as VOC data. Mixing ratios of methane and H_2 were set to be 1.8 ppmV and 550 ppbV. The model was calculated in a time-dependent mode with 5 min time resolution. Each model run started with 3-day spin-up time to reach steady-state conditions for long-lived species. Different scenarios with 1-day, 2-day and 3-day spin-up times have been tried while the differences were within 10 %. Additional loss by dry deposition was assumed to have a corresponding lifetime of 24 h to avoid the accumulation of secondary productions. The boundary layer height was set as constant to 1000 m in the model due to the lack of measurements. This was similar to model setups in Lu et al. (2013) and field measurement results in Guo et al. (2016).

2.3.2 Ozone production efficiency

Ozone production efficiency (OPE) is defined as the number of molecules of total oxidants produced photochemically when a molecule of NO_x was oxidized (Kleinman, 2002; Chou et al., 2011). It helps to evaluate the impacts of VOC reactivity on ozone production in various NO_x regimes. In this work, the OPE was expressed as the ratio of ozone production rate (i.e., $P(O_3)$) to NO_x consumption rate (i.e., $D(NO_x)$). NO_z, calculated as the difference between NO_y (sum of all odd-nitrogen compounds) and NO_x, was assumed to be the oxidation product of NO_x. Thus, the OPE could be also calculated as $P(O_3)/P(NO_z)$. The ozone production rate is obtained as 2–2, and the $P(NO_z)$ is approximately the production rate of HNO_3 and organic nitrate, which is given as (5).

$$P(O_3) = k_{HO_2+NO}[HO_2][NO] + \sum_i k_{RO_{2_i}+NO}\left[RO_{2_i}\right][NO] \quad (5)$$

$$P(NO_z) = k_{NO_2+OH}[NO_2][OH] + \sum_i k_{RO_i+NO_2}[RO_i][NO_2] \quad (6)$$

3 Results

3.1 Time series of meteorology and trace gases

The time series of selected meteorological parameters and inorganic trace gases were presented in 5 min averages (Fig. 5). The median values of the inorganic trace gases were 0.715 ± 0.335 ppmV for CO, 6.3 ± 5.75 ppbV for NO and 36.5 ± 21.3 ppbV for NO_2 and 57 ± 44 ppbV for O_3 in Beijing. In Heshan, the median results were 0.635 ± 0.355 ppmV for CO, 9.7 ± 6.95 ppbV for NO, 29.6 ± 12.6 ppbV for NO_2 and 55.7 ± 34.9 ppbV for O_3. Both sets of results were within the range of data from the literature (Zhang et al., 2008; Zheng et al., 2010; Zhang et al., 2014). However, the daytime averaged O_3 mixing ratio in Beijing in 2013 was a little lower than the median results (about 60 ppbV) in normal years (Zhang et al., 2014). This could be due to higher frequencies of cloudy and rainy days, which accounted for about one-third of our measurement duration. The measured maximum photolysis rates on cloudy/rainy days were about half of the peak values of J (O^1D) on sunny days. Even under these circumstances, ozone levels from the campaign remained high, the pollution episodes with ozone exceeding Grade II of China's National Ambient Air Quality Standard (93 ppbV) occurred quite often, and the percentage of exceedance was 40 % in Beijing and 20 % in Heshan.

The mixing ratios of VOCs in both campaigns were presented in Tables S3 and S4. In the summer in Beijing, alkanes accounted for over 60 % of the summed VOC mixing ratios during most of the time, while in Heshan the contribution from aromatics was 6 % higher than that in Beijing. This could be explained by stronger emissions from solvent use and paint industry in the PRD region (Zheng et al., 2009). The ratio of toluene to benzene, which is typically used qualitatively as an indicator for aromatic emission sources, also supported this assumption. While this ratio in Beijing was

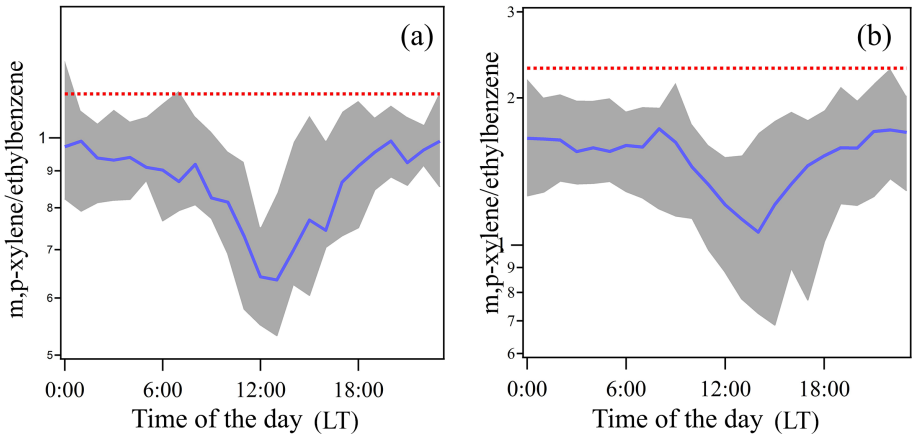

Figure 7. Ratios of m,p-xylene to ethylbenzene in Beijing in 2013 **(a)** and Heshan in 2014 **(b)**. Red dotted line: the highest m,p-xylene to ethylbenzene ratio, assumed as emission ratios of m,p-xylene to ethylbenzene, 1.15 ppbV ppbV^{-1} in Beijing in 2013 **(a)** and 2.3 ppbV ppbV^{-1} in Heshan in 2014 **(b)**. Shaded regions indicate the standard deviation for the ratios during the campaign average.

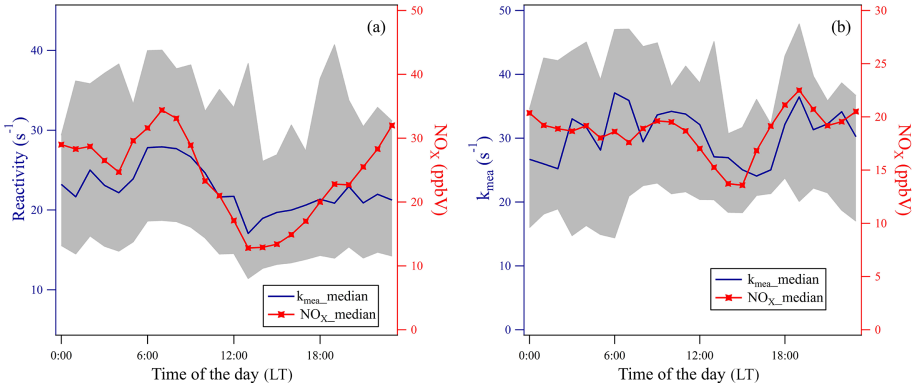

Figure 8. Diurnal variation of hourly median results of measured OH reactivity and NO_x mixing ratios in Beijing **(a)** and Heshan **(b)**.

close to 2, similar to vehicle emissions (Barletta et al., 2005), the ratio in Heshan was higher than 3 due to strict control of benzene in solvent usage in the present day (Barletta et al., 2005; Liu et al., 2008). In the ozone-polluted episode in Fig. 5, the mixing ratios of most species were about 2–3 times higher than the daily average results.

The diurnal variations of NO_x, O_3 and photochemical age from the Beijing and Heshan sites were compared in Figs. 6 and 7. Both sites presented similar diurnal patterns for O_3 and NO. However, the highest 1 h average O_3 value at the PKU site came in the afternoon and stayed at a high level until the dawn, while the O_3 pattern at the Heshan site did not stay high in the afternoon. An additional similarity was that the NO peaks occurred at similar times for both sites. However, NO decreased at a slower rate in Heshan until even 12:00 LT. This was likely explained by the fact that the NO observed at the PKU site was mainly from local vehicle emissions, while NO_x at the Heshan site was significantly influenced by long-range transportation of air masses.

VOC measurements provided us a chance to evaluate the oxidation state at the two sites. Based on the OH exposure calculation methods (de Gouw et al., 2005), we chose a pair of VOC species: m,p-xylene and ethylbenzene to calculate the photochemical age:

$$[\mathrm{OH}]\,\Delta t = \left[\ln\left(\frac{[E]}{[X]}\right)_t - \ln\left(\frac{[E]}{[X]}\right)_0\right]/(k_E - k_X). \quad (7)$$

Here, $[E]$ and $[X]$ represent the mixing ratios of ethylbenzene and m,p-xylene; k_E and k_X indicate the OH reaction rate coefficient of ethylbenzene and m,p-xylene. As presented in Fig. 7, we chose 1.15 and 2.3 ppbV ppbV^{-1} as emission ratios of ethylbenzene to m,p-xylene in Beijing and Heshan, as they were the largest ratios in diurnal variations for the campaign. The largest OH exposure in Beijing in 2013 was calculated as 0.71×10^{11} molecule s cm^{-3} at 13:00 LT, while the largest OH exposure in Heshan in 2014 was calculated to be 1.69×10^{11} molecule s cm^{-3} at 14:00 LT. The results in Beijing were comparable to previous reports (Yuan et al., 2012). Assuming the daytime average ambient OH concentration was 5.2×10^6 molecule cm^{-3} (Lu et al., 2013), the

photochemical age in Beijing was estimated to be not more than 3.5 h. With measured daytime average OH concentration as 7.5×10^6 molecule cm^{-3} in Heshan (Tan et al., unpublished data), the photochemical age in Heshan was about 6 to 7 h, which was about twice the photochemical age of the Beijing observations, indicating a more aged atmospheric environment in Heshan. However, the assumed OH radical concentrations' influence on the photochemical age results should not be neglected.

3.2 Measured reactivity

Total OH reactivity ranged from less than 10 to over 100 s^{-1} in Beijing (Fig. 5a). The daily median value was 20 ± 11 s^{-1}. The diurnal patterns changed significantly from day to day (Fig. 8). The averaged diurnal pattern showed that the total OH reactivity was higher from dawn to morning rush hours, with a peak hourly mean of 27 s^{-1}, and decreased to a lower median value of 17 s^{-1} in the afternoon. This diurnal pattern was similar to the variations of NO_x mixing ratios (Williams et al., 2016).

Meanwhile, measured total OH reactivity in Heshan was higher in median but the diel variation was less evident. The daily median value was 31 ± 20 s^{-1}. The OH reactivity was much less variable in the daily variation. This could possibly be due to the more aged air masses in Heshan, as presented in Sect. 3.1. The other probable explanation could be the two periods of clean air we encountered, during which ground-level ozone and $PM_{2.5}$ concentrations were rather low; each of the cases lasted for about 5 days during our measurements. Additionally, two pollution episodes were identified between 24–27 October and 14–17 November 2014. Both episodes showed accumulation of ozone and $PM_{2.5}$. The total OH reactivity level also built up significantly (Fig. 5b).

3.3 Variations in missing reactivity

Significant differences were found between the measured reactivity and calculated reactivity, which were derived from mixing ratios of different species and multiplied by their rate coefficients with OH radicals, as presented in Fig. 5a for Beijing and Fig. 5b for Heshan. Taking all measured species into consideration, NO_x and NMHCs showed the largest contribution: 45–55 % of total OH reactivity (Fig. 9). The OVOCs also had a significant contribution, and measured OVOCs had a share of 10 % in total reactivity in Beijing while they were 7 % in Heshan.

The missing reactivity was on average over 4 s^{-1} and 21 ± 17 % of the total OH reactivity in Beijing, and 10 s^{-1} and 32 ± 21 % in Heshan. The missing reactivity presented different temporal patterns. In Beijing, the missing reactivities were high during pollution episodes, especially during the morning rush hours. The percentage of missing reactivity could reach over 50 %. For the Heshan site, the missing reactivity was more or less stable during the entire campaign. Even on clean days with reactivity levels lower than 20 s^{-1}, 20–30 % of missing reactivity still existed.

4 Discussion

4.1 Reactivity levels in Beijing and Heshan

The measured VOC reactivity (obtained by subtracting inorganic reactivity from total OH reactivity), 11.2 s^{-1} in Beijing and 18.3 s^{-1} in Heshan (Fig. 10), was actually not high compared to the levels from the literature. Tokyo presented a similar level of VOC reactivity (Yoshino et al., 2006). The measured NMHC levels (obtained by adding all hydrocarbon mixing ratios together) were also not very high, with Beijing in 2013 being around 20 ppbV and Heshan in 2014 higher than 35 ppbV. The relative VOC reactivity values, defined by the ratio of the VOC reactivity to the measured NMHCs levels, for both Beijing and Heshan, were very high.

One possible explanation is the higher content of reactive hydrocarbons in China. Compared to other campaigns, both sites had higher loading of alkenes and aromatics (Yuan et al., 2012; Wang et al., 2014b). The other probable reason is the contribution from OVOCs. In Beijing and Heshan, ambient formaldehyde could accumulate to over 10 ppbV, which was significantly higher than levels found in other observations (Li et al., 2013; Chen et al., 2014). Another possible explanation is unmeasured species, either primary hydrocarbons or secondary products, which will be discussed in later sessions.

4.2 Contributions to the missing reactivity: primary VOCs

As missing reactivity was observed at the Beijing and Heshan sites, the species possibly causing these missing were examined. Throughout the whole campaign at the PKU site, missing reactivity was normally found in the morning, for example, on 16 and 17 August 2013, as shown in Fig. 11. Between 05:00 and 10:00 LT, local vehicle-related sources were strong, and the chemical reactions were not active yet; thus, the oxidant levels and the secondary VOC species remained low. We assumed that the unmeasured primary VOC species could most likely be the major contributors to missing reactivity. Special attention was paid to the unmeasured branched alkenes for their high reactivity, previously observed from vehicle exhaust (Nakashima et al., 2010) and gasoline evaporation emissions (Wu et al., 2015). We found only one dataset of branched alkene measurements in Beijing in 2005 measured by NOAA (Liu et al., 2009). We chose the diurnal patterns of missing reactivity in Beijing in 2013 and compared them to the diel cycles of four measured branched alkenes in 2005. The correlations were found as presented in Fig. 11. Considering the contribution of the four branched alkenes, the VOC reactivity could be enhanced by 2.3 s^{-1}. This could only partially explain the missing VOC reactivity

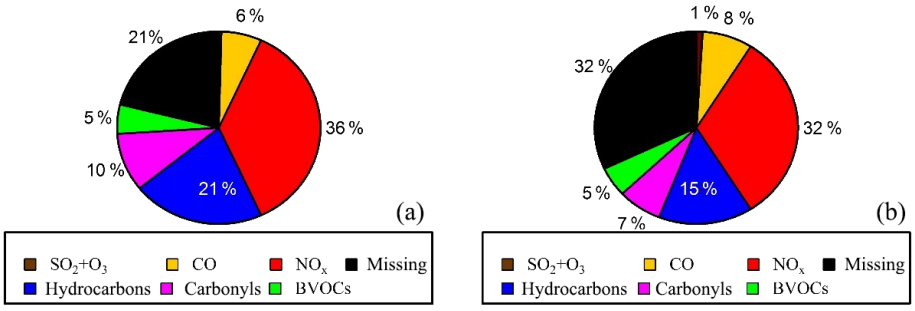

Figure 9. Composition of measured reactivity in Beijing **(a)** and Heshan **(b)**.

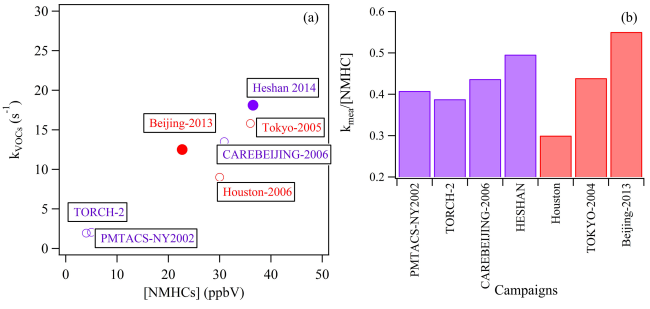

Figure 10. (a) Comparison of VOC reactivity and measured NMHCs in urban and suburban observations. **(b)** Comparison of the ratio between VOC reactivity and measured NMHCs in urban and suburban observations.

which was around $10\,s^{-1}$. With observed decreasing trends in mixing ratios of most NMHC species in Beijing (Zhang et al., 2014; Wang et al., 2015), the branched alkenes were insufficient to tell the full story of the missing reactivity. Unmeasured semivolatile organic compounds (SVOCs) and intermediate volatile organic compounds (IVOCs), such as alkanes between C12 and C30, and polycyclic aromatic hydrocarbons (PAHs) could be also important. Sheehy (2010) found SVOCs and IVOCs contributed to about 10 % during daytime in Mexico City. Future studies with a wider range of reactive VOC measurements for total OH reactivity closure is needed.

4.3 Contributions to the missing reactivity: secondary VOCs

Due to limitations in chemistry mechanisms as well as measuring techniques, secondary products are not fully quantified in ambient air and could probably contribute significantly to the observed missing reactivity, especially in the urban or suburban sites receiving chemically complex aged air masses.

Besides the large missing reactivity during the morning rush hour, there was about a 25 % difference between measured and calculated reactivity from 16 to 18 August 2013 at the PKU site. Considering high levels of oxidants during daytime, the mixing ratios of branched alkenes could be lower than 0.1 ppbV, which could not explain the observed missing reactivity. A box model was deployed to investigate the role of secondary species in variation of VOC reactivity. The model, constrained by measured parameters (meteorology, inorganic gases, VOCs including measured carbonyls), gave the results of VOC reactivity which agreed well with the measured reactivity during most of the daytime (Fig. 11). Major contributors from modeled species were unmeasured aldehydes, glyoxal and methyl glyoxal. Average values of major secondary contributors to modeled reactivity are provided in Table S5. However, the missing reactivity in the morning hours remains unsolved: in the model run, the higher secondary contribution on the morning of 17 August 2013 was due to isoprene oxidation products; by using 1.5 ppbv of isoprene levels as model input, the missing reactivity remained over 40 % around 07:00 and 08:00 LT.

The similar model was applied for the Heshan observation (Fig. 12). During the polluted episode between 24 and 27 October 2014, a 30 % missing reactivity existed for most of the time. Unfortunately, the modeled reactivity was only 10–20 % higher than calculated reactivity and was not enough to explain the measured reactivity. The major contributors among modeled species were also unmeasured aldehydes, glyoxal, methyl glyoxal and other secondary products, as shown in Table S6. Due to strong emissions of aromatics from solvent use and the petroleum industry in the PRD region (Zheng et al., 2009), high levels of glyoxal and methyl glyoxal in this region were observed from satellite measurements (Liu et al., 2012) and ground measurements (Li et al., 2013). Compared to the 2006 measurements in Backgarden, a semirural site in the PRD region, the modeled glyoxal was twice as high as around 0.8 ppbV (Li et al., 2013). This difference possibly resulted from higher levels of precursors in 2014 measurements, where the measured reactivity was about 50 % higher than the results in Backgarden in 2006 (Lou et al., 2010).

4.4 Implications for ozone production efficiency

The investigation of missing VOC reactivity is expected to help better understand the ozone formation processes. To

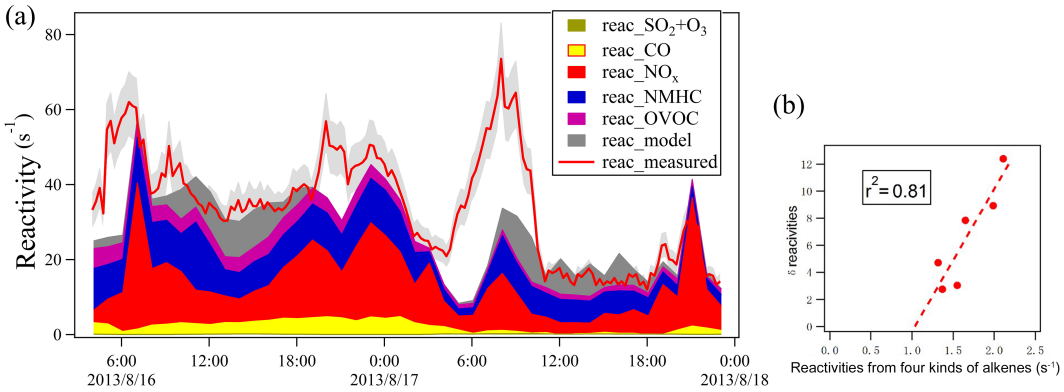

Figure 11. (a) Comparison between measured and calculated reactivity in Beijing from 16 to 18 August 2013. The shallow shaded region indicates uncertainty of measured reactivity. The same shallow shaded region in Fig. 12 represents the same. Panel **(b)** shows the correlation between missing reactivity measured in 2013 and reactivity assumed from branched–chained alkenes from 2005 in diurnal patterns. The four branched alkenes are isobutene, 2-methyl-1-butene, 3-methyl-1-butene and 2-methyl-2-butene.

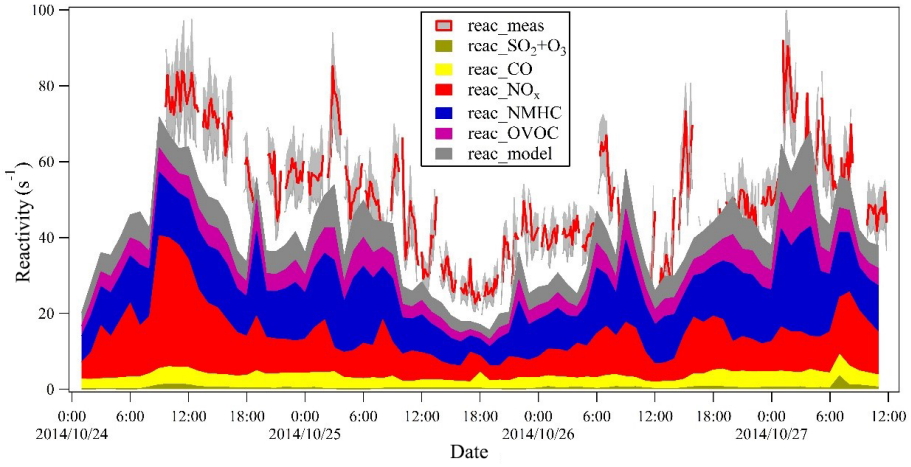

Figure 12. Comparison between measured reactivity and calculated reactivity, as well as modeled reactivity in Heshan between 24 and 27 October 2014.

evaluate this contribution, we employed the box model to calculate the influence of VOC reactivity on OPE. We set two scenarios for the model run. The first was the base run constrained with measured species, including all inorganic compounds, PAMS 56 hydrocarbons, TO-15 OVOCs and formaldehyde. This is how we obtained the modeled reactivity as presented above, and the intermediates and oxidation products were reproduced as well. The other scenario used measured reactivity as a constraint. Due to the difference between measured and modeled reactivity, we allocated the missing reactivity into several groups. For the primary species, we assumed the ratios between total chain alkenes and branched alkenes were the same in Beijing in 2013 and in Heshan in 2014 as the ratio in Beijing 2005, so we got the assumed mixing ratios of branched alkenes at both sites. For secondary species, we allocated the remaining missing reactivity into different intermediates or products based on weights obtained in the model base run. Under both assumptions, we ran the OBM and calculated the OPE, as presented in Fig. 13.

For both sites, the OPE constrained by measured reactivity was significantly higher than the OPE we calculated from modeled reactivity. In Beijing, the OPE from measured reactivity was about 21 % higher on average. The value was 30 % higher at the Heshan site under similar assumptions. This percentage was close to the percentage of missing reactivity, indicating that ignoring unmeasured or unknown organic species can cause significant underestimation in ozone production calculation. When the four branched alkenes were included in the OPE calculation, the OPE results would be 4 % higher than the OPE constrained by calculated reactivity but still far from the OPE constrained by measured reactivity.

Compared to other similar calculations worldwide, the OPE results for Beijing and Heshan were significantly higher (Fig. 14). The comparison was made for $NO_x = 20$ ppbV, which was in the range of most observation results. For urban

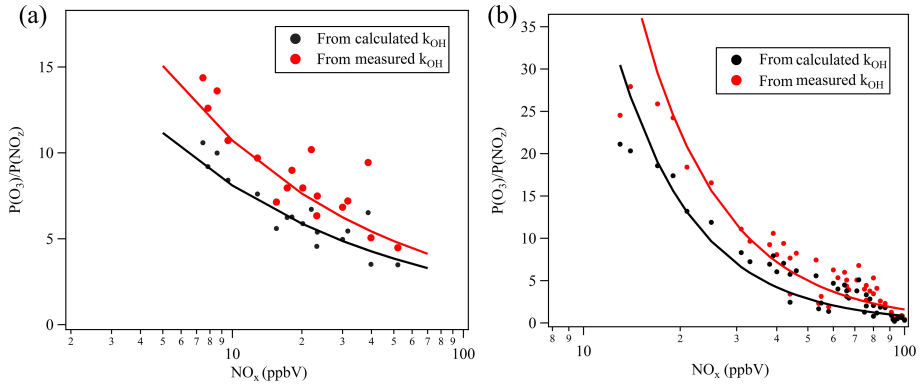

Figure 13. Comparison between OPE calculated from measured reactivity and calculated reactivity in Beijing **(a)** and Heshan **(b)**.

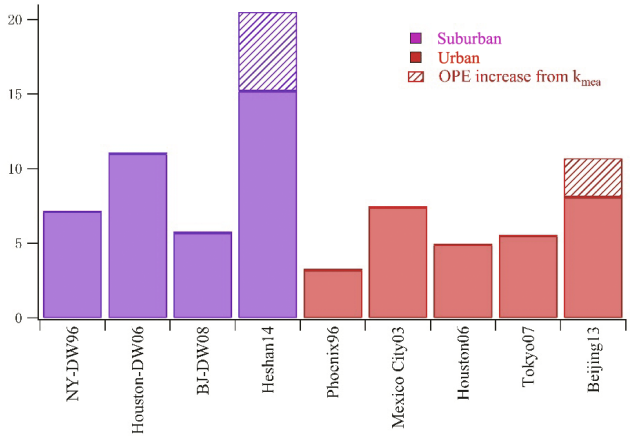

Figure 14. Comparison between the OPE results in this study and other results from the literature. The comparison is made with the $NO_x = 20$ ppbV measurement. DW is the abbreviation for downwind.

measurements, only the results from Mexico City in MCMA-03 were close to the Beijing results in the basic model run (Lei et al., 2008). For suburban measurements, the OPE in Heshan in 2014 was higher than in the other three campaigns, even including the results from the Shangdianzi station in the CAREBeijing-2008 campaign (Ge et al., 2013). While taking missing reactivity into consideration, the OPE results were even higher, indicating more ozone was produced by the reactions of the same quantity of NO_x molecules.

5 Conclusions

In this study, total OH reactivity measurements employing the CRM system were conducted at the PKU site in Beijing in 2013 and the Heshan site in 2014 in the PRD region. Comparisons between measured and calculated reactivity, as well as modeled reactivity, were made and possible reasons for the missing reactivity have been investigated. The contribution of missing reactivity to ozone production efficiency was evaluated.

In Beijing in 2013, the daily median result for measured total OH reactivity was $20 \pm 11\ s^{-1}$. Similar diurnal variation with other urban measurements was found with peaks over $25\ s^{-1}$ during the morning rush hour and lower reactivity than $16\ s^{-1}$ in the afternoon. In Heshan in 2014, total OH reactivity was $31 \pm 20\ s^{-1}$ of the daily median result. The diurnal variation was not significant. Both sites have experienced OH reactivity over $80\ s^{-1}$ during polluted episodes.

Missing reactivity was found at both sites. While in Beijing the missing reactivity made up 21 % of measured reactivity, some periods even reached a higher missing percentage, such as 40–50 %. In Heshan, missing reactivity's contribution to total OH reactivity was 32 % on average and quite stable for the whole day. Unmeasured primary species, such as branched alkenes, could be important contributors to the missing reactivity in Beijing, especially during the morning rush hour, but they were not enough to explain the 17 August morning event. With the help of RACM2, unmeasured secondary products were calculated, and thus the modeled reactivity could agree with measured reactivity in Beijing at noon. However, they were still not enough to explain the missing reactivity in Heshan, even during daytime. This was probably because of the relatively higher oxidation stage in Heshan than in Beijing.

Missing reactivity could impact the estimation of atmospheric ozone production efficiency. Compared to modeled reactivity from the base run, ozone production efficiency would rise 21 and 30 % in Beijing and Heshan with measured reactivity applied. Both results were significantly higher than similar observations worldwide, indicating the relatively faster ozone production at both sites.

However, in order to further explore the OH reactivity in both regions, more efforts should be paid in both OH reactivity measurements and speciated measurements, as well as modeling to close the total OH reactivity budget. Moreover, a thorough way with more detailed mechanisms should be es-

tablished to connect the missing reactivity to the evaluation of ozone production.

Data availability. The data used in this study are available from the corresponding author upon request (mshao@pku.edu.cn).

The Supplement related to this article is available online at https://doi.org/10.5194/acp-17-7127-2017-supplement.

Competing interests. The authors declare that they have no conflict of interest.

Acknowledgements. This study was funded by the National Key Research and Development Plan (grant no. 2016YFC020200), Natural Science Foundation for Outstanding Young Scholars (grant no. 41125018) and a Natural Science Foundation key project (grant no. 411330635). The research was also supported by the European Commission Partnership with China on Space Data (PANDA project). The authors give special thanks to Jing Zheng, Mei Li and Yuhan Liu from Peking University and Tao Zhang from the Guangdong Environmental Monitoring Center for their help and give thanks to William C. Kuster from the NOAA Earth System Research Laboratory for the branched-alkene data from 2005.

Edited by: D. Heard
Reviewed by: three anonymous referees

References

Barletta, B., Meinardi, S., Sherwood Rowland, F., Chan, C.-Y., Wang, X., Zou, S., Yin Chan, L., and Blake, D. R.: Volatile organic compounds in 43 Chinese cities, Atmos. Environ., 39, 5979–5990, https://doi.org/10.1016/j.atmosenv.2005.06.029, 2005.

Calpini, B., Jeanneret, F., Bourqui, M., Clappier, A., Vajtai, R., and van den Bergh, H.: Direct measurement of the total reaction rate of OH in the atmosphere, Analusis, 27, 328–336, https://doi.org/10.1051/analusis:1999270328, 1999.

Chatani, S., Shimo, N., Matsunaga, S., Kajii, Y., Kato, S., Nakashima, Y., Miyazaki, K., Ishii, K., and Ueno, H.: Sensitivity analyses of OH missing sinks over Tokyo metropolitan area in the summer of 2007, Atmos. Chem. Phys., 9, 8975–8986, https://doi.org/10.5194/acp-9-8975-2009, 2009.

Chen, W. T., Shao, M., Lu, S. H., Wang, M., Zeng, L. M., Yuan, B., and Liu, Y.: Understanding primary and secondary sources of ambient carbonyl compounds in Beijing using the PMF model, Atmos. Chem. Phys., 14, 3047–3062, https://doi.org/10.5194/acp-14-3047-2014, 2014.

Chou, C. C.-K., Tsai, C.-Y., Chang, C.-C., Lin, P.-H., Liu, S. C., and Zhu, T.: Photochemical production of ozone in Beijing during the 2008 Olympic Games, Atmos. Chem. Phys., 11, 9825–9837, https://doi.org/10.5194/acp-11-9825-2011, 2011.

de Gouw, J. A., Middlebrook, A. M., Warneke, C., Goldan, P. D., Kuster, W. C., Roberts, J. M., Fehsenfeld, F. C., Worsnop, D. R., Canagaratna, M. R., Pszenny, A. A. P., Keene, W. C., Marchewka, M., Bertman, S. B., and Bates, T. S.: Budget of organic carbon in a polluted atmosphere: Results from the New England Air Quality Study in 2002, J. Geophy. Res.-Atmos., 110, D16305, https://doi.org/10.1029/2004jd005623, 2005.

Dodge, M. C.: Proceedings of the international conference on photochemical oxidant pollution and its control, Combined use of modeling techniques and smog chamber data to derive ozone-precursor relationships, US Environmental Protection Agency, Research Triangle Park, NC, 881–889, 1977.

Dolgorouky, C., Gros, V., Sarda-Esteve, R., Sinha, V., Williams, J., Marchand, N., Sauvage, S., Poulain, L., Sciare, J., and Bonsang, B.: Total OH reactivity measurements in Paris during the 2010 MEGAPOLI winter campaign, Atmos. Chem. Phys., 12, 9593–9612, https://doi.org/10.5194/acp-12-9593-2012, 2012.

Edwards, P. M., Evans, M. J., Furneaux, K. L., Hopkins, J., Ingham, T., Jones, C., Lee, J. D., Lewis, A. C., Moller, S. J., Stone, D., Whalley, L. K., and Heard, D. E.: OH reactivity in a South East Asian tropical rainforest during the Oxidant and Particle Photochemical Processes (OP3) project, Atmos. Chem. Phys., 13, 9497–9514, https://doi.org/10.5194/acp-13-9497-2013, 2013.

Fang, X., Shao, M., Stohl, A., Zhang, Q., Zheng, J., Guo, H., Wang, C., Wang, M., Ou, J., Thompson, R. L., and Prinn, R. G.: Top-down estimates of benzene and toluene emissions in the Pearl River Delta and Hong Kong, China, Atmos. Chem. Phys., 16, 3369–3382, https://doi.org/10.5194/acp-16-3369-2016, 2016.

Fuchs, H., Hofzumahaus, A., Rohrer, F., Bohn, B., Brauers, T., Dorn, H. P., Häseler, R., Holland, F., Kaminski, M., Li, X., Lu, K., Nehr, S., Tillmann, R., Wegener, R., and Wahner, A.: Experimental evidence for efficient hydroxyl radical regeneration in isoprene oxidation, Nat. Geosci., 6, 1023–1026, https://doi.org/10.1038/ngeo1964, 2013.

Ge, B. Z., Sun, Y. L., Liu, Y., Dong, H. B., Ji, D. S., Jiang, Q., Li, J., and Wang, Z. F.: Nitrogen dioxide measurement by cavity attenuated phase shift spectroscopy (CAPS) and implications in ozone production efficiency and nitrate formation in Beijing, China. J. Geophy. Res.-Atmos., 118, 9499–9509, https://doi.org/10.1002/jgrd.50757, 2013.

Geddes, J. A., Murphy, J. G., and K., W. D.: Long term changes in nitrogen oxides and volatile organic compounds in Toronto and the challenges facing local ozone control, Atmos. Environ., 43, 3407–3415, https://doi.org/10.1016/j.atmosenv.2009.03.053, 2009.

Geiger, H., Barnes, I., Bejan, I., Benter, T., and Spittler, M.: The tropospheric degradation of isoprene: an updated module for the regional atmospheric chemistry mechanism, Atmos. Environ., 37, 1503–1519, https://doi.org/10.1016/S1352-2310(02)01047-6, 2003.

Goliff, W. S., Stockwell, W. R., and Lawson, C. V.: The regional atmospheric chemistry mechanism, version 2, Atmos. Environ., 68, 174–185, https://doi.org/10.1016/j.atmosenv.2012.11.038, 2013.

Guo, J., Miao, Y., Zhang, Y., Liu, H., Li, Z., Zhang, W., He, J., Lou, M., Yan, Y., Bian, L., and Zhai, P.: The climatology of planetary boundary layer height in China derived from radiosonde and reanalysis data, Atmos. Chem. Phys., 16, 13309–13319, https://doi.org/10.5194/acp-16-13309-2016, 2016.

Hansen, R. F., Blocquet, M., Schoemaecker, C., Léonardis, T., Locoge, N., Fittschen, C., Hanoune, B., Stevens, P. S., Sinha, V.,

and Dusanter, S.: Intercomparison of the comparative reactivity method (CRM) and pump-probe technique for measuring total OH reactivity in an urban environment, Atmos. Meas. Tech., 8, 4243–4264, https://doi.org/10.5194/amt-8-4243-2015, 2015.

Ingham, T., Goddard, A., Whalley, L. K., Furneaux, K. L., Edwards, P. M., Seal, C. P., Self, D. E., Johnson, G. P., Read, K. A., Lee, J. D., and Heard, D. E.: A flow-tube based laser-induced fluorescence instrument to measure OH reactivity in the troposphere, Atmos. Meas. Tech., 2, 465–477, https://doi.org/10.5194/amt-2-465-2009, 2009.

Karl, M., Dorn, H.-P., Holland, F., Koppmann, R., Poppe, D., Rupp, L., Schaub, A., and Wahner, A.: Product study of the reaction of OH radicals with isoprene in the atmosphere simulation chamber SAPHIR, J. Atmos. Chem., 55, 167–187, https://doi.org/10.1007/s10874-006-9034-x, 2006.

Kato, S, Sato, T., and Kaji, Y.: A method to estimate the contribution of unidentified VOCs to OH reactivity, Atmos. Environ., 45, 5531–5539, doi:10.1016/j.atmosenv.2011.05. 074. 2011.

Kleinman, L. I.: Ozone production efficiency in an urban area, J. Geophys. Res.-Atmos., 107, D234733, https://doi.org/10.1029/2002jd002529, 2002.

Kovacs, T. A. and Brune, W. H.: Total OH loss rate measurement, J. Atmos. Chem., 39, 105–122, https://doi.org/10.1023/a:1010614113786, 2001.

Kovacs, T. A., Brune, W. H., Harder, H., Martinez, M., Simpas, J. B., Frost, G. J., Williams, A. G., Jobson, B. T., Stroud, C., Young, V., Fried, A., and B., W.: Direct measurements of urban OH reactivity during Nashville SOS in summer 1999, J. Environ. Monit., 5, 68–74, https://doi.org/10.1039/b204339d, 2003.

Kumar V. and Sinha, V.: VOC-OHM: a new technique for rapid measurements of ambient total OH reactivity and volatile organic compounds using a single proton transfer reaction mass spectrometer, Int. J. Mass Spectrom., 374, 55–63, 2014.

LaFranchi, B. W., Goldstein, A. H., and Cohen, R. C.: Observations of the temperature dependent response of ozone to NO_x reductions in the Sacramento, CA urban plume, Atmos. Chem. Phys., 11, 6945–6960, https://doi.org/10.5194/acp-11-6945-2011, 2011.

Lee, J. D., Young, J. C., Read, K. A., Hamilton, J. F., Hopkins, J. R., Lewis, A. C., Bandy, B. J., Davey, J., Edwards, P. M., Ingham, T., Self, D. E., Smith, S. C., Pilling, M. J., and Heard, D. E.: Measurement and calculation of OH reactivity at a United Kingdom coastal site, J. Atmos. Chem., 64, 53–76, https://doi.org/10.1007/s10874-010-9171-0, 2010.

Lei, W., Zavala, M., de Foy, B., Volkamer, R., and Molina, L. T.: Characterizing ozone production and response under different meteorological conditions in Mexico City, Atmos. Chem. Phys., 8, 7571–7581, https://doi.org/10.5194/acp-8-7571-2008, 2008.

Li, M., Shao, M., Li, L.-Y., Lu, S.-H., Chen, W.-T., and Wang, C.: Quantifying the ambient formaldehyde sources utilizing tracers, Chinese, Chem. Lett., 25, 1489–1491, https://doi.org/10.1016/j.cclet.2014.07.001, 2014.

Li, X., Brauers, T., Hofzumahaus, A., Lu, K., Li, Y. P., Shao, M., Wagner, T., and Wahner, A.: MAX-DOAS measurements of NO_2, HCHO and CHOCHO at a rural site in Southern China, Atmos. Chem. Phys., 13, 2133–2151, https://doi.org/10.5194/acp-13-2133-2013, 2013.

Liu, Y., Shao, M., Fu, L., Lu, S., Zeng, L., and Tang, D.: Source profiles of volatile organic compounds (VOCs) measured in China: Part I, Atmos. Environ., 42, 6247–6260, https://doi.org/10.1016/j.atmosenv.2008.01.070, 2008.

Liu, Y., Shao, M., Kuster, W. C., Goldan, P. D., Li, X. H., Lu, S. H., and de Gouw, J. A.: Source identification of reactive hydrocarbons and oxygenated VOCs in the summertime in Beijing, Environ. Sci. Technol., 43, 75–81, https://doi.org/10.1021/es801716n, 2009.

Liu, Y. H., Lu, K. D., Dong, H. B., Li, X., Cheng, P., Zou, Q., Wu, Y. S., Liu, X. G., and Zhang, Y. H.: In situ monitoring of atmospheric nitrous acid based on multi-pumping flow system and liquid waveguide capillary cell, J. Envion. Sci., 43, 273–284, https://doi.org/10.1016/j.jes.2015.11.034, 2016.

Liu, Z., Wang, Y., Vrekoussis, M., Richter, A., Wittrock, F., Burrows, J. P., Shao, M., Chang, C.-C., Liu, S.-C., Wang, H., and Chen, C.: Exploring the missing source of glyoxal (CHOCHO) over China, Geophy. Res. Lett., 39, L10812, https://doi.org/10.1029/2012gl051645, 2012.

Lou, S., Holland, F., Rohrer, F., Lu, K., Bohn, B., Brauers, T., Chang, C. C., Fuchs, H., Häseler, R., Kita, K., Kondo, Y., Li, X., Shao, M., Zeng, L., Wahner, A., Zhang, Y., Wang, W., and Hofzumahaus, A.: Atmospheric OH reactivities in the Pearl River Delta – China in summer 2006: measurement and model results, Atmos. Chem. Phys., 10, 11243–11260, https://doi.org/10.5194/acp-10-11243-2010, 2010.

Lu, K. D., Zhang, Y. H., Su, H., Brauers, T., Chou, C. C., Hofzumahaus, A., Liu, S. C., Kita, K., Kondo, Y., Shao, M., Wahner, A., Wang, J. L., Wang, X., and T., Z.: Oxidant (O_3+ NO_2) production processes and formation regimes in Beijing, J. Geophys. Res.-Atmos., 115, D07303, https://doi.org/10.1029/2009jd012714, 2010.

Lu, K. D., Hofzumahaus, A., Holland, F., Bohn, B., Brauers, T., Fuchs, H., Hu, M., Häseler, R., Kita, K., Kondo, Y., Li, X., Lou, S. R., Oebel, A., Shao, M., Zeng, L. M., Wahner, A., Zhu, T., Zhang, Y. H., and Rohrer, F.: Missing OH source in a suburban environment near Beijing: observed and modelled OH and HO_2 concentrations in summer 2006, Atmos. Chem. Phys., 13, 1057–1080, https://doi.org/10.5194/acp-13-1057-2013, 2013.

Mao, J. Q., Ren, X. R., Chen, S., Brune, W. H., Chen, Z., Martinez, M., Harder, H., Lefer, B., Rappengluck, B., Flynn, J., and Leuchner, M.: Atmospheric oxidation capacity in the summer of Houston 2006: Comparison with summer measurements in other metropolitan studies, Atmos. Environ., 44, 4107–4115, https://doi.org/10.1016/j.atmosenv.2009.01.013, 2010.

Michoud, V., Hansen, R. F., Locoge, N., Stevens, P. S., and Dusanter, S.: Detailed characterizations of the new Mines Douai comparative reactivity method instrument via laboratory experiments and modeling, Atmos. Meas. Tech., 8, 3537–3553, https://doi.org/10.5194/amt-8-3537-2015, 2015.

Nakashima, Y., Kamei, N., Kobayashi, S., and Y., K.: Total OH reactivity and VOC analyses for gasoline vehicular exhaust with a chassis dynamometer, Atmos. Environ., 44, 468–475, https://doi.org/10.1016/j.atmosenv.2009.11.006, 2010.

Nölscher, A. C., Williams, J., Sinha, V., Custer, T., Song, W., Johnson, A. M., Axinte, R., Bozem, H., Fischer, H., Pouvesle, N., Phillips, G., Crowley, J. N., Rantala, P., Rinne, J., Kulmala, M., Gonzales, D., Valverde-Canossa, J., Vogel, A., Hoffmann, T., Ouwersloot, H. G., Vilà-Guerau de Arellano, J., and Lelieveld, J.: Summertime total OH reactivity measurements from boreal

forest during HUMPPA-COPEC 2010, Atmos. Chem. Phys., 12, 8257–8270, https://doi.org/10.5194/acp-12-8257-2012, 2012.

Nölscher, A. C., Yanez-Serrano, A. M., Wolff, S., de Araujo, A. C., Lavric, J. V., Kesselmeier, J., and Williams, J.: Unexpected seasonality in quantity and composition of Amazon rainforest air reactivity, Nat. commun., 7, 10383–10394, https://doi.org/10.1038/ncomms10383, 2016.

Pöschl, U., von Kuhlmann, R., Poisson, N., and Crutzen, P. J.: Development and intercomparison of condensed isoprene oxidation mechanisms for global atmospheric modeling, J. Atmos. Chem., 37, 29–52, https://doi.org/10.1023/A:1006391009798, 2000.

Ren, X. R., Harder, H., Martinez, M., Lesher, R. L., Oliger, A., Shirley, T., Adams, J., Simpas, J. B., and H., B. W.: HO_x concentrations and OH reactivity observations in New York City during PMTACS-NY2001, Atmos. Environ., 37, 3627–3637, https://doi.org/10.1016/s1352-2310(03)00460-6, 2003.

Ren, X. R., Brune, W. H., Cantrell, C., Edwards, G. D., Shirley, T., Metcalf, A. R., and Lesher, L. R.: Hydroxyl and Peroxy Radical Chemistry in a Rural Area of Central Pennsylvania: Observations and Model Comparisons, J. Atmos. Chem., 52, 231–257, https://doi.org/10.1007/s10874-005-3651-7, 2005.

Ren, X. R., Brune, W. H., Mao, J. Q., Mitchell, M. J., Lesher, R. L., Simpas, J. B., Metcalf, A. R., Schwab, J. J., Cai, C., and Li, Y. Q., Demerjian, K. L., Felton, H. D., Boynton, G., Adams, A., Perry, J., He, Y, Zhou, X. L., and Hou, J.: Behavior of OH and HO_2 in the winter atmosphere in New York City, Atmos. Environ. 40, 252–263, https://doi.org/10.1016/j.atmosenv.2005.11.073, 2006a.

Ren, X. R., Brune, W. H., Oliger, A., Metcalf, A. R., Simpas, J. B., Shirley, T., Schwab, J. J., Bai, C., Roychowdhury, U., Li, Y., Cai, C., Demerjian, K. L., He, Y., Zhou, X. H., Gao, H., and Hou, J.: OH, HO_2, and OH reactivity during the PMTACS–NY Whiteface Mountain 2002 campaign: Observations and model comparison, J. Geophys. Res.-Atmos., 111, 6126–6137, https://doi.org/10.1029/2005jd006126, 2006b.

Sadanaga, Y., Yoshino, A., Kato, S., Yoshioka, A., Watanabe, K., Miyakawa, T., Hayashi, I., Ichikawa, M., Matsumoto, J., Nishiyama, A., Akiyama, N., Kanaya, Y., and Y., K.: The importance of NO_2 and volatile organic compounds in the urban air from the viewpoint of the OH reactivity, Geophys. Res. Lett., 31, L08102, https://doi.org/10.1029/2004gl019661, 2004.

Sadanaga, Y., Yoshino, A., Kato, S., and Y., K.: measurements of OH reactivity and photochemical ozone production in the urban atmosphre, Environ. Sci. Technol., 39, 8847–8852, https://doi.org/10.1021/es049457p, 2005.

Sheehy, P. M., Volkamer, R., Molina, L. T., and Molina, M. J.: Oxidative capacity of the Mexico City atmosphere – Part 2: A RO_x radical cycling perspective, Atmos. Chem. Phys., 10, 6993–7008, https://doi.org/10.5194/acp-10-6993-2010, 2010.

Shirley, T. R., Brune, W. H., Ren, X. R., Mao, J. Q., Lesher, R., Cardenas, B., Volkamer, R., Molina, L. T., Molina, M. J., Lamb, B., Velasco, E., Jobson, T., and M., A.: Atmospheric oxidation in the MCMA during April 2003, Atmos. Chem. Phys., 6, 2753–2765, https://doi.org/10.5194/acp-6-2753-2006, 2006.

Sinha, V., Williams, J., Crowley, J. N., and Lelieveld, J.: The Comparative Reactivity Method – a new tool to measure total OH Reactivity in ambient air, Atmos. Chem. Phys., 8, 2213–2227, https://doi.org/10.5194/acp-8-2213-2008, 2008.

Sinha, V., Custer, T. G., Kluepfel, T., and Williams, J.: The effect of relative humidity on the detection of pyrrole by PTR-MS for OH reactivity measurements, Int. J. Mass Spectrom., 282, 108–111, https://doi.org/10.1016/j.ijms.2009.02.019, 2009.

Sinha, V., Williams, J., Lelieveld, J., Ruuskanen, T. M., Kalos, M. K., Patokoski, L., Hellen, H., Hakola, H., Mogensen, D., Boy, M., Rinne, L., and M., K.: OH reactivity measurements within a boreal forest – evidence for unknown reactive emissions, Environ. Sci. Technol., 44, 6614–6620, https://doi.org/10.1021/es101780b, 2010.

Sinha, V., Williams, J., Diesch, J. M., Drewnick, F., Martinez, M., Harder, H., Regelin, E., Kubistin, D., Bozem, H., Hosaynali-Beygi, Z., Fischer, H., Andrés-Hernández, M. D., Kartal, D., Adame, J. A., and Lelieveld, J.: Constraints on instantaneous ozone production rates and regimes during DOMINO derived using in-situ OH reactivity measurements, Atmos. Chem. Phys., 12, 7269–7283, https://doi.org/10.5194/acp-12-7269-2012, 2012.

Stockwell, W. R., Kirchner, F., Kuhn, M., and Seefeld, S.: A new mechanism for regional atmospheric chemistry modeling, J. Geophys. Res.-Atmos., 102, 25847–25879, https://doi.org/10.1029/97jd00849, 1997.

Stone, D., Whalley, L. K., and Heard, D. E.: Tropospheric OH and HO_2 radicals: field measurements and model comparisons, Chem. Soc. Rev., 41, 6348–6404, https://doi.org/10.1039/c2cs35140d, 2012.

Wang, M., Zeng, L., Lu, S., Shao, M., Liu, X., Yu, X., Chen, W., Yuan, B., Zhang, Q., Hu, M., and Zhang, Z.: Development and validation of a cryogen-free automatic gas chromatograph system (GC-MS/FID) for online measurements of volatile organic compounds, Anal. Methods, 6, 9424–9434, https://doi.org/10.1039/c4ay01855a, 2014a.

Wang, M., Shao, M., Chen, W., Yuan, B., Lu, S., Zhang, Q., Zeng, L., and Wang, Q.: A temporally and spatially resolved validation of emission inventories by measurements of ambient volatile organic compounds in Beijing, China, Atmos. Chem. Phys., 14, 5871–5891, https://doi.org/10.5194/acp-14-5871-2014, 2014b.

Wang, M., Shao, M., Chen, W., Lu, S., Liu, Y., Yuan, B., Zhang, Q., Zhang, Q., Chang, C. C., Wang, B., Zeng, L., Hu, M., Yang, Y., and Li, Y.: Trends of non-methane hydrocarbons (NMHC) emissions in Beijing during 2002–2013, Atmos. Chem. Phys., 15, 1489–1502, https://doi.org/10.5194/acp-15-1489-2015, 2015.

Wang, T., Ding, A., Gao, J., and Wu, W. S.: Strong ozone production in urban plumes from Beijing, China, Geophy. Res. Lett., 33, L21806, https://doi.org/10.1029/2006gl027689, 2006.

Whalley, L. K., Stone, D., Bandy, B., Dunmore, R., Hamilton, J. F., Hopkins, J., Lee, J. D., Lewis, A. C., and Heard, D. E.: Atmospheric OH reactivity in central London: observations, model predictions and estimates of in situ ozone production, Atmos. Chem. Phys., 16, 2109–2122, https://doi.org/10.5194/acp-16-2109-2016, 2016.

Williams, J.: Provoking the air, Environ. Chem., 5, 317–319, https://doi.org/10.1071/en08048, 2008.

Williams, J. and Brune, W. H.: A roadmap for OH reactivity research, Atmos. Environ., 106, 371–372, https://doi.org/10.1016/j.atmosenv.2015.02.017, 2015.

Williams, J., Keßel, S. U., Nölscher, A. C., Yang, Y. D., Lee, Y. N., Yáñez-Serrano, A. M., Wolff, S., Kesselmeier, J., Klüpfel, T., Lelieveld, J., and Shao, M.: Opposite OH

reactivity and ozone cycles in the Amazon rainforest and megacity Beijing: Subversion of biospheric oxidant control by anthropogenic emissions, Atmos. Environ., 125, 112–118, https://doi.org/10.1016/j.atmosenv.2015.11.007, 2016.

Wu, Y., Yang, Y. D., Shao, M., and Lu, S. H.: Missing in total OH reactivity of VOCs from gasoline evaporation, Chinese, Chem. Lett., 26, 1246–1248, https://doi.org/10.1016/j.cclet.2015.05.047, 2015.

Yang, Y., Shao, M., Wang, X., Nölscher, A. C., Kessel, S., Guenther, A., and Williams, J.: Towards a quantitative understanding of total OH reactivity: A review, Atmos. Environ., 134, 147–161, https://doi.org/10.1016/j.atmosenv.2016.03.010, 2016.

Yoshino, A., Sadanaga, Y., Watanabe, K., Kato, S., Miyakawa, Y., Matsumoto, J., and Kajii, Y.: Measurement of total OH reactivity by laser-induced pump and probe technique – comprehensive observations in the urban atmosphere of Tokyo, Atmos. Environ., 40, 7869–7881, https://doi.org/10.1016/j.atmosenv.2006.07.023, 2006.

Yoshino, A., Nakashima, Y., Miyazaki, K., Kato, S., Suthawaree, J., Shimo, N., Matsunaga, S., Chatani, S., Apel, E., Greenberg, J., Guenther, A., Ueno, H., Sasaki, H., Hoshi, J., Yokota, H., Ishii, K., and Kajii, Y.: Air quality diagnosis from comprehensive observations of total OH reactivity and reactive trace species in urban central Tokyo, Atmos. Environ., 49, 51–59, https://doi.org/10.1016/j.atmosenv.2011.12.029, 2012.

Yuan, B., Shao, M., de Gouw, J., Parrish, D. D., Lu, S., Wang, M., Zeng, L., Zhang, Q., Song, Y., Zhang, J., and Hu, M.: Volatile organic compounds (VOCs) in urban air: How chemistry affects the interpretation of positive matrix factorization (PMF) analysis, J. Geophys. Res.-Atmos., 117, D24302, https://doi.org/10.1029/2012jd018236, 2012.

Zhang, Q., Yuan, B., Shao, M., Wang, X., Lu, S., Lu, K., Wang, M., Chen, L., Chang, C. C., and Liu, S. C.: Variations of ground-level O_3 and its precursors in Beijing in summertime between 2005 and 2011, Atmos. Chem. Phys., 14, 6089–6101, https://doi.org/10.5194/acp-14-6089-2014, 2014.

Zhang, Y. H., Su, H., Zhong, L. J., Cheng, Y. F., Zeng, L. M., Wang, X. S., Xiang, Y. R., Wang, J. L., Gao, D. F., and Shao, M.: Regional ozone pollution and observation-based approach for analyzing ozone–precursor relationship during the PRIDE-PRD2004 campaign, Atmos. Environ., 42, 6203–6218, https://doi.org/10.1016/j.atmosenv.2008.05.002, 2008.

Zhao, C., Wang, Y. H., and Zeng, T.: East China Plains: a "Basin" of ozone pollution, Environ. Sci. Technol., 43, 1911–1915, https://doi.org/10.1021/es8027764, 2009.

Zhao, W., Cohan, D. S., and Henderson, B. H.: Slower ozone production in Houston, Texas following emission reductions: evidence from Texas Air Quality Studies in 2000 and 2006. Atmos. Chem. Phys. 14, 2777–2788, https://doi.org/10.5194/acp-14-2777-2014, 2014.

Zheng, J. Y., Shao, M., Che, W. W., Zhang, L. J., Zhong, L. J., Zhang, Y. H., and Streets, D.: Speciated VOC emission inventory and spatial patterns of ozone formation potential in the Pearl River Delta, China, Environ. Sci. Technol. 43, 8580–8586, https://doi.org/10.1021/es901688e, 2009.

Zheng, J. Y., Zhong, L. J., Wang, T., Louie, P. K. K., and Li, Z. C.: Ground-level ozone in the Pearl River Delta region: analysis of data from a recently established regional air quality monitoring network, Atmos. Environ., 44, 814–823, https://doi.org/10.1016/j.atmosenv.2009.11.032, 2010.